Iranian Journal of Microbiology
*Volume 18 Number 4 (August 2026) 533-543*
DOI: http://doi.org/10.18502/ijm.v18i4.22196

ORIGINAL ARTICLE

# Surveying a *Pseudomonas aeruginosa*-derived oxidoreductase activity

**Maliheh Mohammadkhani[1], Shamsozoha Abolmaali[2*], Shakiba Darvishalipour Astaneh[1]**

*[1]Department of Biotechnology, Faculty of New Sciences and Technologies, Semnan University, Semnan, Iran*
*[2]Department of Biology, Faculty of Basic Science, Semnan University, Semnan, Iran*

**Received:** September 2023**, Accepted:** July 2026

## ABSTRACT

**Background and Objectives:** Flavoprotein monooxygenases (FPMOs) participate in various biological processes, including lignin degradation, natural product biosynthesis, and xenobiotic detoxification. This study aimed to investigate the heterologous expression of FPMO and assess its functional activity by examining its capacity to inactivate ampicillin.

**Materials and Methods:** *In silico* analyses were performed to predict the enzyme's secondary and tertiary structures. The target gene was isolated from *Pseudomonas aeruginosa*, cloned into the pET-22b vector, and expressed in *Escherichia coli* BL21 (DE3). Heterologous protein expression was examined using SDS–PAGE, and the protein was purified through nickel-affinity chromatography. Enzymatic activity was measured by spectrophotometric monitoring of NADPH oxidation at 340 nm. Antibacterial activity was tested using an agar well-diffusion assay, measuring the inhibition zone diameter in *E. coli* treated with ampicillin.

**Results:** Homology modeling indicated that the 3D structure of FPMO is very similar to cyclohexanone monooxygenase, supporting its classification as a Baeyer–Villiger monooxygenase (BVMO). Molecular docking proposed that ampicillin might be a substrate for FPMO, with predicted interactions at Ile141 and Val159. Enzymatic assays confirmed that FPMO catalyzes the oxidation of ampicillin, using FAD and NADPH as cofactors. Additionally, well-diffusion tests showed decreased ampicillin antibacterial activity after treatment. The enzyme's activity was further confirmed using an ampicillin inactivation assay.

**Conclusion:** The heterologously expressed protein was functionally active. These findings suggest that the studied FPMO may play a role in antibiotic resistance in *P. aeruginosa* by oxidatively inactivating ampicillin.

**Keywords:** Ampicillin; Flavoprotein; Oxidoreductase; *Pseudomonas aeruginosa*

## INTRODUCTION

*Pseudomonas aeruginosa* causes hospital-acquired infections and is a major pathogen in lung infections among patients with cystic fibrosis (1). Its remarkable ability to develop resistance to multiple classes of antibiotics has made *P. aeruginosa* a significant global public health threat. Accordingly, the World Health Organization (WHO) has included carbapenem-resistant *P. aeruginosa* in its Bacterial Priority Pathogens List, highlighting the urgent need for new antimicrobial therapies (2). Recent evidence shows that the high prevalence of drug-resistant strains is partly due to inadequate treatment of susceptible populations, including improper antibiotic use and suboptimal dosing (3). Antibiotic resistance in *P. aeruginosa* can be either inherent or acquired, with key mechanisms involving efflux

*Corresponding author: Shamsozoha Abolmaali, Ph.D, Department of Biology, Faculty of Basic Science, Semnan University, Semnan, Iran. Tel: +98-2331532288; +98-91277319460 Fax: +98-2333654110 Email: s_abolmaali@semnan.ac.ir

pumps and antibiotic-inactivating enzymes. Among these, β-lactamases—classified into four molecular classes (A–D)—are important because they hydrolyze the β-lactam ring and inactivate the antibiotic (4, 5). Many studies have examined the distribution of β-lactamase genes in Gram-negative clinical isolates to understand resistance patterns in healthcare settings (6). Beyond β-lactamases, there is growing interest in flavin-dependent monooxygenases (FMOs) as contributors to antibiotic resistance. TetX, a flavin-dependent monooxygenase, confers tetracycline resistance by breaking down tetracyclines (7). Similarly, rifampicin monooxygenases enable the hydroxylation of rifampicin, rendering it inactive. The FMO Rif-Orf17 has been shown to catalyze a dual-oxidation reaction that degrades and inactivates rifamycin SV (8, 9). Additionally, Kim et al. (2019) demonstrated that co-expression of flavin reductase and sulfonamide monooxygenases (sulX and sul1) increases sulfonamide resistance in *Acinetobacter* spp. (10).

FMOs are versatile enzymes involved in various metabolic processes, such as the breakdown of aromatic compounds, the production of polyketides, siderophores, cholesterol, and antibiotics, and the regulation of antibiotic resistance mechanisms (11). Studies show that microbial FMOs share catalytic properties with their eukaryotic counterparts; however, they are often preferred as biocatalysts because of their solubility and ease of recombinant production (12). Sequence analyses place FMOs within the class B flavoprotein monooxygenase family, which is widely found in bacteria and fungi. Many of these enzymes belong to the Baeyer–Villiger monooxygenase (BVMO) subfamily, which catalyzes Baeyer–Villiger oxidations and plays a role in primary and secondary metabolism through producing bioactive compounds (13). Structurally, BVMOs have distinct binding domains for FAD and NADPH, with NAD(P)H remaining associated with the enzyme during catalysis. Despite conserved functional domains, small differences in sequence motifs give this enzyme family a broad range of substrate specificities (9). Unlike human FMOs, microbial BVMOs are usually soluble and suitable for recombinant production. For example, eight class B flavoprotein monooxygenases from *Rhodococcus jostii* RHA1 have been cloned and studied for their roles in oxidation and sulfoxidation (14). The PA4991 protein of *P. aeruginosa*, a putative FAD-dependent oxidoreductase, has been reported to act on various amino acid substrates and may help bacteria survive in the sputum of cystic fibrosis patients receiving antibiotic treatment. This suggests a possible role in inactivating antibiotics (15).

*P. aeruginosa* naturally resists ampicillin and other β-lactam and non-β-lactam antibiotics. The MuxABC-OpmB efflux system, a member of the resistance–nodulation–division (RND) family, confers resistance to ampicillin and carbenicillin and increases bacterial pathogenicity. Evidence indicates that ampicillin resistance in *P. aeruginosa* mainly results from reduced membrane permeability and active efflux. Although β-lactamases are known to deactivate ampicillin, the potential involvement of FMO enzymes in this process remains uncertain (16). In this study, we examined the role of an FAD-dependent monooxygenase (FPMO) in inactivating ampicillin through both computational and experimental methods. Our results suggest that this enzyme could be a target for the development of treatments against ampicillin-resistant *P. aeruginosa*.

## MATERIALS AND METHODS

**Bacterial strains, plasmids, and reagents.** Genomic DNA from *P. aeruginosa* (ATCC 27853) was used to amplify the gene encoding an FAD-dependent oxidoreductase (locus A4W92_15705). *E. coli* BL21(DE3) as the expression host and pET-22b(+) as the expression vector were chosen. Restriction enzymes (*BamH*I and *Xho*I) and IPTG (Merck) were obtained from Sinaclon (Tehran, Iran). NADPH and FAD were purchased from Sigma-Aldrich. Cells were cultured in Luria–Bertani (LB) broth supplemented with 100 μg/mL ampicillin.

**Cloning, expression, purification, and western blot analysis of FPMO.** Genomic DNA was extracted from *P. aeruginosa* as previously described. The gene encoding the FAD-dependent oxidoreductase from *P. aeruginosa* (referred to as FPMO) was amplified via polymerase chain reaction (PCR) using primers FP1 (5′-AGCGGATCCCATGACCGACCTGAATCGCACC-3′) and R1P (5′-GCACTCGAGTCAGCTGACTTCCTGGAGGCTGGTTTG-3′), which include *BamH*I and *Xho*I restriction sites at their 5′ ends, respectively. Primer sequences were manually designed and then validated using Gene Runner software. PCR was performed with an initial

denaturation at 95°C for 3 minutes, followed by 30 cycles of denaturation at 95°C for 45 seconds, annealing at 50°C for 45 seconds, and extension at 72°C for 90 seconds. A final extension step was conducted at 72°C for 10 minutes. The amplified FPMO gene was purified and ligated into the pET-22b(+) expression vector downstream of a 6×His tag using *BamH*I and *Xho*I sites. The heterologous plasmid pET22b-FPMO (pMM9) was transformed into *E. coli* BL21(DE3) by heat shock at 42°C for 90 seconds. Transformants were selected on LB agar plates containing 100 µg/mL ampicillin ($LB_{Amp}$).

LB-Amp was inoculated with an overnight culture of *E. coli* BL21(DE3) carrying pMM9 and incubated at 37°C, at 180 rpm until the optical density at 620 nm ($OD_{620}$) reached about 0.6. Heterologous protein expression was induced by adding isopropyl β-D-1-thiogalactopyranoside (IPTG) to a final concentration of 1 mM, followed by incubation at 22°C for 20 hours. To optimize FPMO expression, the effects of IPTG concentration, induction temperature, and induction time were systematically tested. IPTG concentrations of 0.1, 0.5, 0.7, and 1.0 mM were examined at induction temperatures of 16, 22, 25, 30, and 37°C and induction periods of 4.5, 10, 16, and 24 hours.

Following induction, cells were pelleted by centrifugation at 8,000 × g, 15 minutes at 4°C, then resuspended in lysis buffer containing 50 mM Tris-HCl, 300 mM NaCl, and 10 mM imidazole (pH 8.0). The cell suspension was kept on ice for 30 minutes, then sonicated for 7 cycles of 15 seconds at 4°C. Cellular debris was removed by centrifugation at 8,000 × g for 15 minutes at 4°C, and the clarified lysate was used for protein purification.

Heterologous $His_6$-tagged FPMO was purified under native conditions using Ni-NTA affinity chromatography. Briefly, 2.5 mL of Ni-NTA agarose resin (QIAGEN) was equilibrated with lysis buffer before loading. An aliquot (600 µL) of clarified lysate was applied to the column, followed by washing with 600 µL of wash buffer (50 mM Tris-HCl, 300 mM NaCl, and 10 mM imidazole, pH 8.0). Bound proteins were eluted with an imidazole gradient from 20 to 250 mM. 12% SDS-PAGE was used to analyze protein expression and purification, and protein identity was further confirmed by Western blot analysis. Purified FPMO was separated by 12% SDS-PAGE, then electrotransferred onto a nitrocellulose membrane at 70 V for 2 hours at 4°C. Protein transfer was verified by staining the membrane with Ponceau S solution for 20 minutes, followed by rinsing with distilled water. The membrane was then blocked overnight at 4°C in blocking buffer containing 5% (w/v) skim milk in PBST. Subsequently, the membrane was washed three times with PBST for 10 minutes each at room temperature and incubated for 1 hour at 20°C with an anti-His-tag antibody diluted 1:2500 in PBST. After three additional washes with PBST, immunoreactive bands were detected using 3,3′-diaminobenzidine (DAB) substrate solution activated with 15 µL $H_2O_2$. The reaction was terminated by rinsing the membrane with distilled water once the desired signal intensity was reached (17).

**Enzyme activity assay.** FPMO activity was measured by two methods: (i) spectrophotometric detection of NADPH oxidation at 340 nm and (ii) testing the antibacterial activity of enzyme-treated ampicillin against *E. coli*.

For the spectrophotometric assay, reactions were carried out in a total volume of 200 µL containing 50 mM Tris–HCl buffer (pH 8.0), 100 µM NADPH, 0.7 mg $mL^{-1}$ purified FPMO, and 2.8 mM ampicillin. The reaction was initiated by adding NADPH and continuously monitored for 1 min by measuring the decrease in absorbance at 340 nm ($\varepsilon_{340}$ = 6.22 $mM^{-1}$ $cm^{-1}$), which indicates NADPH oxidation. One unit (U) of enzyme activity was defined as the amount of enzyme required to oxidize 1 µmol of NADPH per minute under the assay conditions (18, 19). All enzyme assays were performed at 25°C in triplicate using independent biological replicates. Enzyme activity was calculated from the rate of decrease in absorbance at 340 nm over time. Negative control reactions were prepared under identical conditions but without the enzyme. Protein concentration was determined using the Bradford assay, with bovine serum albumin (BSA) as the standard.

**Antibacterial activity assay.** The effect of FPMO treatment on ampicillin's antibacterial activity was assessed using an agar well-diffusion assay. Reaction mixtures containing 2.8 mM ampicillin, 0.1 mM NADPH, and 0.7 mg/mL purified FPMO in 50 mM Tris–HCl buffer were incubated at room temperature for 30 minutes in a final volume of 200 µL. Control reactions were prepared under the same conditions but without NADPH to prevent enzymatic activity.

Following incubation, 100 µL of each reaction mixture was used to test antibacterial activity against *E.*

*coli* (BL21). *E. coli* BL21 was spread onto the plate surface to achieve a density equivalent to a 0.5 McFarland standard. An 8-mm-diameter well was created in the plate. Aliquots of the reaction mixtures were added to the wells, and the plates were incubated at 37°C for 16 hours. Antibacterial activity was evaluated by measuring the diameter of the growth inhibition zone before and after enzymatic ampicillin treatment. Enzyme activity units (AU) were calculated as previously described (20).

FPMO activity ($mm^2/ml$) = (Lz – Ls)/V

Lz = Clear zone area $(mm)^2$, Ls = Well area $(mm)^2$,

V = Volume of sample (ml)

**Amino acid sequence analysis and secondary structure prediction of FPMO.** The amino acid sequence of FPMO was obtained from NCBI under the accession AMX88367. EXPASY ProtParam (www.expasy.ch/tools) was used to analyze the protein's physicochemical properties, including molecular weight, amino acid composition, and instability index. FPMO signal peptides were predicted using the SignalP 5.0 Server (http://www.cbs.dtu.dk/services/SignalP/). Domain and motif analyses were performed using the MotifFinder, MotifScan, and FingerPRINT tools. The subcellular localization of the enzyme was estimated using PSORTb and PROTTER (http://wlab.ethz.ch/protter/start/). PSIPRED, based on PSI-BLAST (Position-Specific Iterative BLAST), was used as a simple and accurate method for secondary-structure prediction.

**Homology modeling of FPMO and refinement and quality assessment of the protein model.** Homology modeling of FPMO was conducted using the SWISS-MODEL server. The amino acid sequence of FPMO, provided in FASTA format, was searched against the SWISS-MODEL Template Library (SMTL) to identify suitable structural templates. Template selection involved using both BLAST and HHblits. Candidate templates were chosen based on criteria such as high sequence identity, maximum query coverage, high alignment score, and low E-value. Three-dimensional models were generated for each selected template to evaluate structural similarity and conserved regions between the target and template proteins. Model quality was initially assessed using SWISS-MODEL's internal metrics, including the QMEAN scoring function, which provides both global and local estimates of model reliability.

The top-performing model, based on these quality metrics, was further refined using the ModRefiner server (https://zhanglab.ccmb.med.umich.edu/ModRefiner/). Structural validation of the refined model was performed with multiple tools, including Verify3D, ERRAT, the Ramachandran plot server (https://zlab.umassmed.edu/bu/rama/), and the ProSA web server (https://prosa.services.came.sbg.ac.at/prosa.php), to evaluate stereochemical quality and overall structural reliability.

**Molecular docking and ligand interaction studies.** The candidate ligand, ampicillin (PubChem CID: 6249), was retrieved from the PubChem database (https://pubchem.ncbi.nlm.nih.gov/) for docking studies with FPMO. Molecular docking was conducted in the Molecular Operating Environment (MOE) using the optimized protein structure. Hydrogen-bond network optimization (Protonate3D) and energy minimization were performed using the QuickPrep module. The protein's active site was identified using the MOE Site Finder tool. Ampicillin was then docked into the ligand-binding site of FPMO with the MOE-Dock module. Docking parameters included the Triangle Matcher placement method, the AMBER99 molecular mechanics force field, and the London ΔG scoring function for rescoring. Considering structural factors, the simultaneous docking of three molecules—ampicillin, NADPH (coenzyme), and FAD (cofactor)—was evaluated. Binding free energies for each ligand were calculated based on MOE docking scores. Protein–ligand interactions were analyzed using the Ligand Interaction module within MOE, including identification of interaction types, bonding features, and 2D and 3D visualizations of the complexes, along with measurements of distances between ligand and protein atoms. Visualization of molecular structures and interactions was further enhanced using Discovery Studio Visualizer (https://www.chemcomp.com/MOEMolecular_Operating_Environment.htm).

## RESULTS

**Heterologous expression of FPMO and FPMO activity.** The cloning of the FPMO gene was confirmed by sequencing analysis and submitted to NCBI under the accession number OR083140. PCR ampli-

fication further verified the construct, yielding a 1353 bp product. Additionally, the heterologous plasmid pET22b-FPMO was confirmed by restriction enzyme digestion using *BamH*I and *Xho*I (Fig. 1a). SDS-PAGE analysis demonstrated the expression of the heterologous FPMO (pMM9) with an approximate molecular weight of 46 kDa (Fig. 1b). The expressed protein was then purified to a final concentration of 0.7 mg/mL (Fig. 1c). Additionally, the production of FPMO was verified by Western blot analysis (Fig. 1d).

Enzyme activity was measured using two methods. NADPH consumption, which acts as a cofactor, stabilized after about 12 minutes (Fig. 2). Enzyme activity was determined by the decrease in NADPH concentration, resulting in a calculated activity of 3.125 U for FPMO. Additionally, enzyme activity was assessed through a bacterial growth inhibition test.

Antibiotic-sensitive bacteria were exposed to ampicillin before and after treatment with the heterologous enzyme. After 16 hours of incubation, the inhibition zone diameter was 30 mm for the control and 10 mm for the enzyme-treated plate (Fig. 3). Based on the reduction in the inhibition zone diameter, the activity of FPMO against ampicillin was calculated to be 6280 AU.

**Physicochemical properties and sequence analysis.** The enzyme's physicochemical properties were analyzed using ProtParam. The FPMO protein has a molecular weight of 49.53 kDa and comprises 450 amino acids, including 59 negatively charged and 50 positively charged residues, resulting in an overall net negative charge. The instability index was calculated at 37.21, indicating the protein is stable. The aliphatic index was 82.18, suggesting high thermostability. The grand average of hydropathicity (GRAVY) was -0.37, showing a hydrophilic nature and favorable interaction with water. SignalP analysis confirmed the absence of a signal peptide in FPMO. Motif analysis

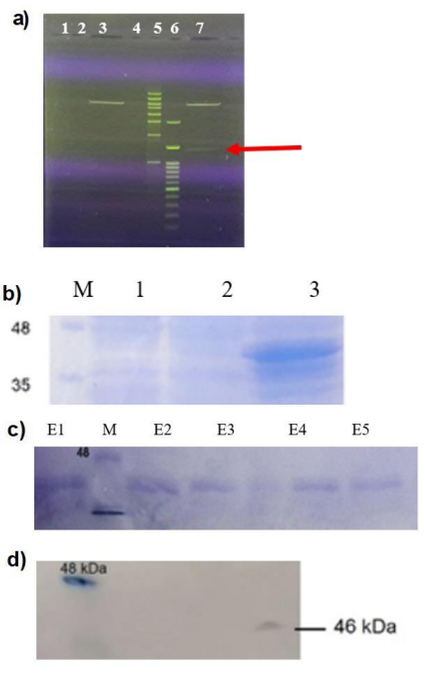


**Fig. 1.** The heterologous plasmid pET22b-FPMO was confirmed by restriction enzyme digestion using *BamH*I and *Xho*I. (3) plasmid pET22b (5) Ladder DNA 1kb (6) Ladder DNA 100 bp (7) pET22b-FPMO (a); Electrophoresis of recombinant FPMO on 12% acrylamide gel under native (1), noninduced (2), and induced (3) cells of *E. coli* BL21-pMM9, respectively. M: protein molecular weight marker 250 kDa (b); The FPMO purification by affinity chromatography on 12% acrylamide gel. Lane description: protein molecular weight marker 250 kDa (M), The SDS-PAGE presents the elution fractions 1 to 6 in the concentrations of 100, 150, 200, and 250 mM imidazole elution buffer (c); Western blot analysis of recombinant FPMO (d).

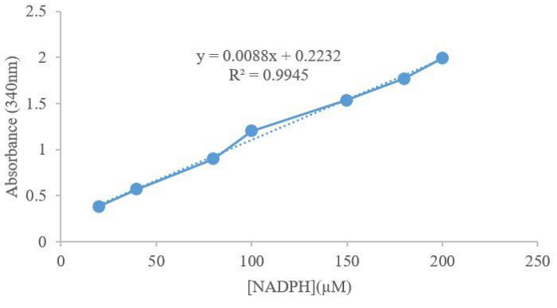


**Fig. 2.** Oxidation of NADPH treated with FPMO, NADPH standard curve at 340 nm.

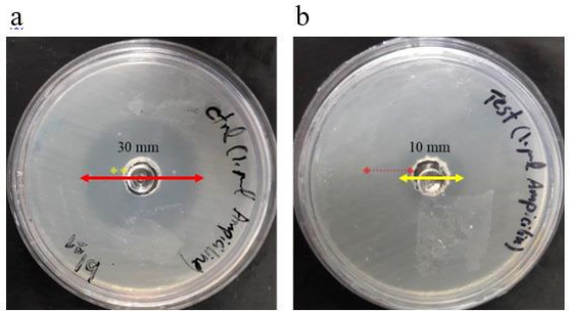


**Fig. 3.** Evaluation of *E. coli* BL21 susceptibility to ampicillin before and after enzymatic treatment a: Control plate (ampicillin); b: Test plate (FPMO-treated ampicillin))

using MotifFinder, Motif Scan, and FingerPRINT identified two conserved GXGXXG Rossmann fold motifs, GAGQAG (associated with FAD binding) and GAGSSG (associated with NADPH binding), along with the characteristic FMO motif EXIXXXHXXXY (ERIRQIHSAHY). These motifs are located in the N-terminal region and are highly conserved functional domains. Subcellular localization prediction with PSORTb, based on bacterial parameters and the FPMO amino acid sequence, indicated cytoplasmic localization with a high confidence score of 9.97. Secondary structure prediction was carried out using PSIPRED (Fig. 4a).

**Homology modeling and model quality evaluation.** The three-dimensional structure was generated using the homology-based modeling program SWISS-MODEL. The final model is shown in Fig. 4b. The best model was built using chain A of the crystal structure 4USR from *Pseudomonas stutzeri* as a template, determined at a resolution of 1.83 Å. Sequence alignment between FPMO and the template revealed 98% coverage and 35% identity. The resulting model received a QMEAN score of 0.66 (range: 0–1), indicating acceptable structural reliability.

The quality of the predicted model was further assessed using multiple validation tools. ProSA-web analysis showed a Z-score of −6.38 (Fig. 5a and b), indicating that the overall model quality is comparable to native protein structures of similar size. Ramachandran plot analysis revealed that 94.03% of residues were in favored regions, 5.22% in allowed regions, and 0.74% in disallowed regions (Fig. 5c), indicating stereochemical quality. ERRAT analysis produced an overall quality factor of 56.0%, while Verify3D indicated that 86.1% of residues had an average 3D–1D score ≥ 0.2, confirming the acceptable reliability of the modeled structure.

**Molecular docking.** Docking analysis of FPMO was conducted using the MOE Simulate module. The most accurate homology model was selected for docking experiments. Multiple binding conformations were evaluated based on their binding affinities and interaction profiles. The docking results from MOE are summarized in Table 1, highlighting the key amino acid residues involved in enzyme–ligand interactions. The enzyme-ampicillin docking yielded a binding score of −11.114 kcal/mol, indicating a strong interaction.

**Ampicillin and FPMO interaction.** Interactions between the FPMO protein and its ligands were analyzed using MOE software. These analyses provided detailed insights into the atomic-level interactions between the protein and each ligand. The most representative 2D and 3D interaction models are shown in Fig. 6.

Docking analysis of NADPH showed that several amino acid residues, including Gly161, Arg139, Ser165, Arg137, Ser143, and His142, are involved in ligand binding within FPMO. Ser143 forms an H interaction at a distance of 3.85 Å, while His142 interacts with the ligand at 3.74 Å (Fig. 6a and b). For FAD, three main interactions were identified: hydrogen bonds with Glu154 and Arg139, an ionic interaction with Arg139, and an H interaction with Val160 within the active site (Fig. 6c and d). Ampicillin binds through hydrogen bonds with Ile141 and Val159, along with an H interaction with Tyr146 at a distance of 3.6 Å (Fig. 6e and f).

## DISCUSSION

*Pseudomonas aeruginosa* is a major cause of healthcare-associated infections due to its innate and acquired resistance to many antibiotics. In this study, we cloned and characterized a flavin-containing monooxygenase from *P. aeruginosa*, a Baeyer–Villiger monooxygenase (BVMO), to explore its potential role in the degradation of ampicillin, a β-lactam antibiotic. Before 2003, research on the catalytic and mechanistic properties of BVMOs mainly focused on cyclohexanone monooxygenase (CHMO) (21). This enzyme has since been widely studied for various biocatalytic applications (22). A new BVMO, 4-hydroxyacetophenone monooxygenase (HAPMO), was identified in *Pseudomonas fluorescens* ACB, with its gene cloned in 2001 (23). Monooxygenases were also implicated in the biosynthesis of alkyl quinolones in *P. aeruginosa*, underscoring their biological significance (24). Although this study emphasizes ampicillin inactivation by FPMO, flavin-containing monooxygenases are known for their broad catalytic versatility. Some FMOs catalyze the oxidation of environmental compounds like skatole, demonstrating their ability to act on diverse substrates, including clinically relevant antibiotics (25).

Protein expression conditions are essential for producing an active enzyme. While recombinant FPMO

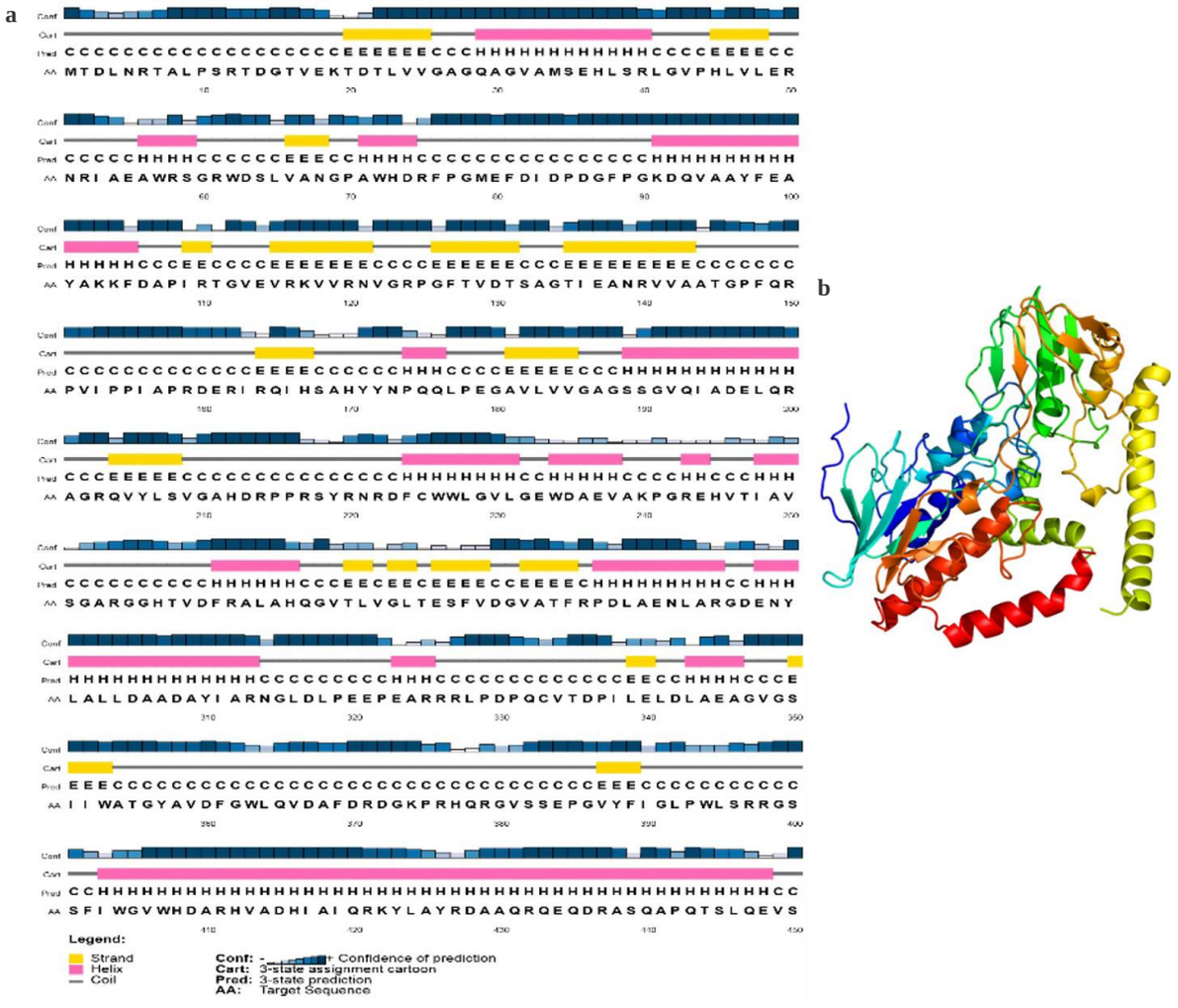


**Fig. 4.** The second and third predicted structures of FPMO and the secondary structure of FPMO using PSIPRED (a); 3D structure prediction of FPMO (b).

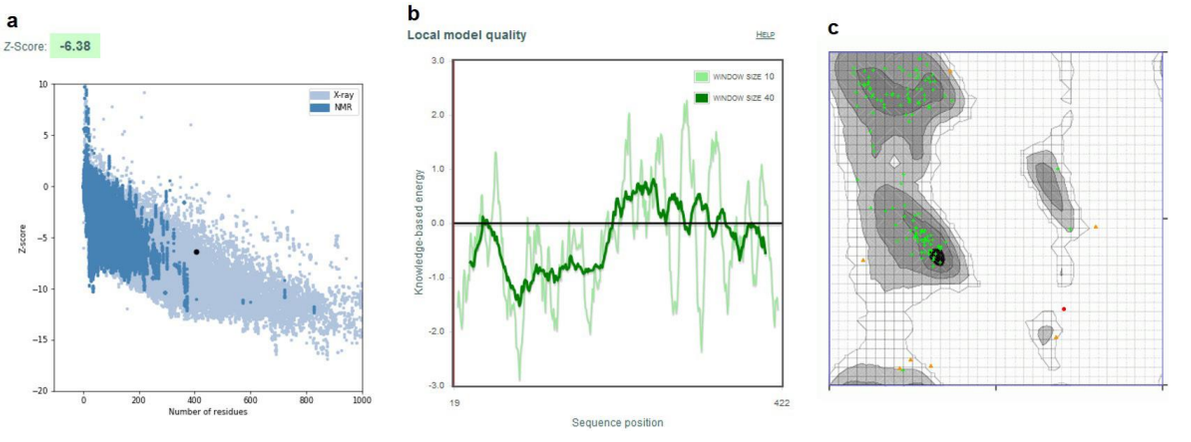


**Fig. 5.** Assessing the quality of the FPMO structure. ProSA-web analysis of FPMO shows the black point indicates the input-modeled FPMO falls within the Z-score range of experimental structures based on amino acid residue count (a); Energy plot of the predicted FPMO (b); Ramachandran plot of the refined FPMO generated by homology modeling (c).

**Table 1.** Docking scores, binding sites, and ligands in FPMO using the MOE program

| Ligand number | Name | PubChem CID | MOE score (Kcal/mol) | Conventional hydrogen bond | pi-H pi-pi pi-cation |
|---|---|---|---|---|---|
| 1 | NADPH | 5884 | -17.950 | Gly161, Arg139, Ser165, Arg137 | Ser143, His142 |
| 2 | FAD | 643975 | -21.558 | Glu154, Arg139 | Val160 |
| 3 | Ampicillin | 6249 | -11.114 | Ile141, Val159 | Tyr146 |

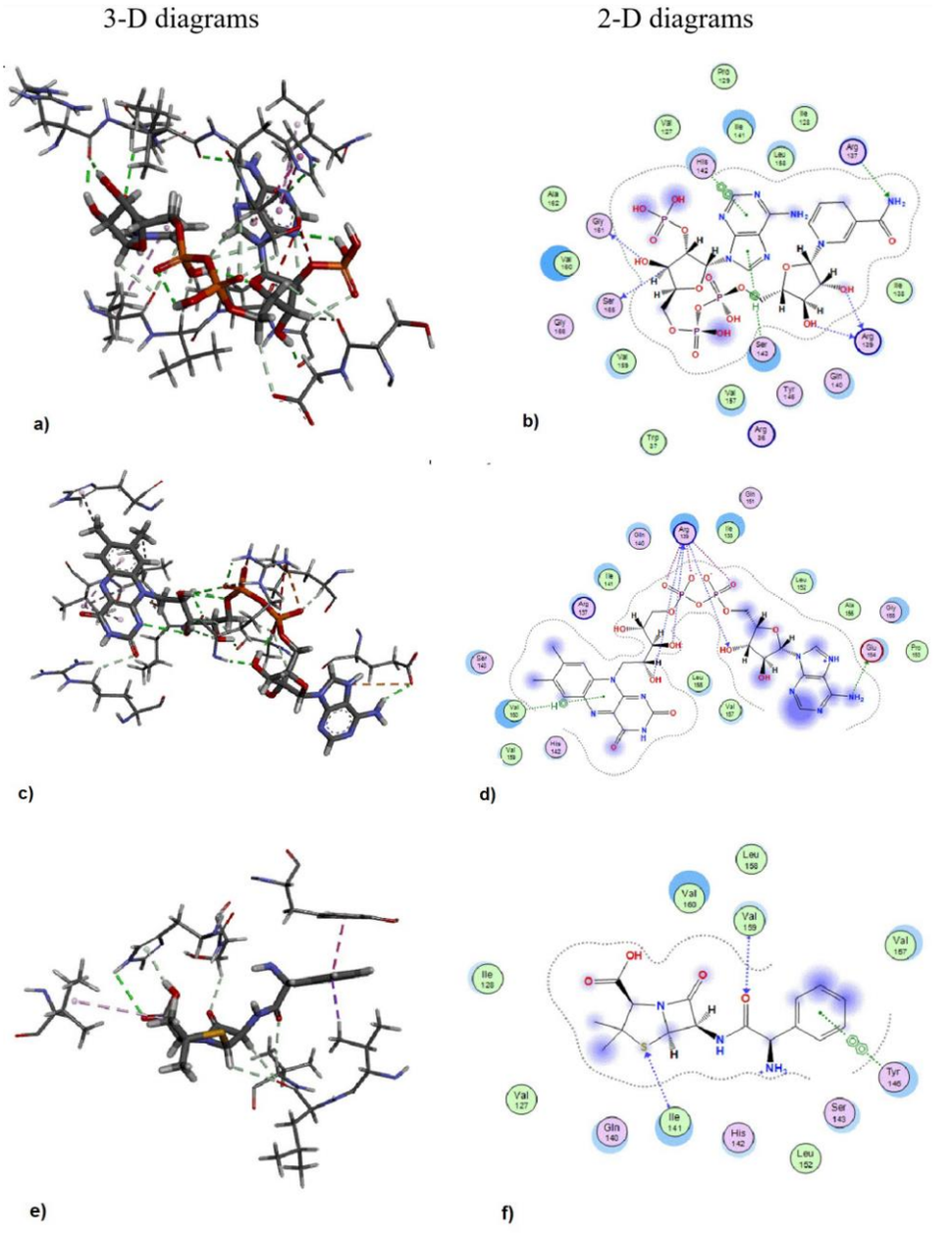


**Fig. 6.** Docking assay analyzing how the FPMO enzyme from *P. aeruginosa* ATCC 27853 interacts with its ligands. The 3D diagrams illustrate FPMO's interactions with NADPH (a), FAD (c), and Ampicillin (e). Meanwhile, the 2D diagrams present the contacts between amino acid residues in FPMO's active sites and these ligands: NADPH (b), FAD (d), and ampicillin (f). Residue types and interaction details are presented in (g).

can be expressed at high levels at 37°C, previous research often reports better folding and activity at lower temperatures (below 25°C). In this study, induction at 22°C improved proper protein folding, likely due to slower cell growth and enhanced folding kinetics (26). Although CHMO shows limited activity when expressed in *E. coli*, alternative hosts such as Pichia pastoris have been shown to increase both yield and catalytic efficiency (27, 9). Additionally, riboflavin-auxotrophic strains such as *E. coli* RBO_AI offer advantages for producing apo-flavoproteins and reducing metabolic load compared with traditional BL21 (DE3) systems, indicating promising directions for future FPMO research (28).

Purification of recombinant FMOs generally involves multiple chromatographic steps, during which enzyme inactivation can occur, often due to unsuitable temperature conditions. Although most FMOs are purified at 4°C to preserve stability and reduce proteolysis, some reports mention successful purification at room temperature. In this study, all purification steps were carried out at 4°C to maintain enzyme activity (29).

Flavin monooxygenases catalyze various oxidative reactions, including N-oxidation, S-oxidation, and Baeyer–Villiger oxidation (30).

These enzymes contain conserved sequence motifs, such as a Rossmann fold for binding FAD and NADPH. Based on sequence and structural analyses, the studied FPMO shares features with type I BVMOs, including similarities to CHMO. This suggests a catalytic mechanism involving a flavin C4a-(hydro)peroxide intermediate that can nucleophilically attack the substrate. Bioinformatic predictions and experimental data in this study confirm that ampicillin is a substrate for FPMO.

Flavoenzymes, including tetracycline deacetylases such as TetX, rely on FAD as a cofactor to catalyze substrate oxidation. TetX catalyzes the breakdown of tetracycline through an oxygen- and NADPH-dependent process. Recent research has revealed new binding modes of tetracycline deacetylases and identified inhibitors targeting the FAD cofactor, helping restore the effectiveness of antibiotics. These findings highlight the broader importance of flavin-dependent enzymes in antibiotic resistance.

Previous reports have also shown that BVMOs and related enzymes can modify antibiotics. For example, Ar-BVMO has been shown to influence imipenem activity through a novel resistance mechanism (31). Rifampicin monooxygenase performs the first hydroxylation step in rifamycin breakdown, while flavin-dependent monooxygenases have been associated with sulfonamide resistance in *Acinetobacter*. A clinical *P. aeruginosa* (Pa-3) strain harbored a gene encoding a Tet(X7)-like enzyme and showed resistance to multiple antibiotics, underscoring the clinical significance of these enzymes (32).

This study evaluated the effect of recombinant FPMO on ampicillin susceptibility in *E. coli* BL21 (DE3). Disk diffusion assays showed reduced antibacterial activity after enzyme treatment, suggesting that FPMO mediates ampicillin modification. Additionally, the enzyme remained active at 37°C, indicating thermal stability under physiological conditions. These findings suggest that FPMO could be a valuable target for strategies to reduce β-lactam resistance in *Pseudomonas.*

However, confirming antibiotic degradation requires directly identifying reaction products. Techniques such as liquid chromatography–high-resolution mass spectrometry (LC–HRMS), which were not available in this study, should be used in future research to analyze degradation intermediates and clarify the specific biochemical pathway (25).

Structural analysis revealed that the FPMO active site is located near the FAD- and NADPH-binding domains and contains conserved arginine residues that are often involved in BVMO catalysis. However, studies on CHMO indicate that not all oxidative activities rely on the conserved arginine residue (33). The active site structure of FPMO appears flexible, potentially enabling it to accommodate a wide range of substrates (34). Although BVMOs often share less than 40% sequence identity, their structural frameworks are highly similar. Comparative modeling with a related structure (PDB ID: 5nmw) revealed differences in cofactor-binding residues between FPMO and related enzymes, although key residues such as glutamate and arginine are conserved. In this study, residues like arginine, serine, isoleucine, and valine were identified as potentially important for substrate interaction. Meanwhile, recent reports highlight the roles of aspartate and arginine in BVMO function (29).

Although this study provides both experimental and computational evidence supporting FPMO's role in ampicillin modification, several limitations should be recognized. First, antibiotic inactivation was inferred indirectly through NADPH consumption and

reduced antibacterial activity, without directly identifying degradation products. Second, kinetic parameters such as Km, kcat, and catalytic efficiency were not measured, which limits understanding of substrate specificity. Third, experiments were conducted in a recombinant *E. coli* system rather than in the native *P. aeruginosa* environment, requiring further validation under physiological conditions. Additionally, molecular docking results offer predictive insights but need experimental confirmation. Finally, only ampicillin was tested, and the substrate scope of FPMO toward other antibiotics remains to be explored. These limitations point to key directions for future research to fully understand the biochemical role and clinical importance of FPMO in antibiotic resistance.

## CONCLUSION

An oxidoreductase from *P. aeruginosa*, with a 3D structure similar to cyclohexanone monooxygenase, was studied for its effect on ampicillin. Docking experiments confirmed that ampicillin is a substrate and identified key positions of Ile141 and Val159 in the FPMO enzyme. Treatment with FPMO inactivated ampicillin, as evidenced by the clear zone in the diffusion test against *E. coli* (BL21). Further enzyme characteristics are being studied and will be reported in the future.

## ACKNOWLEDGEMENTS

The authors acknowledge the Deputy for Research and Technology, Semnan University (Semnan, Iran) for supporting this study. Dr. Taghi Lashkarbolouki and Dr. Noushin Bijari are appreciated for the critical review of the manuscript.

## REFERENCES

1. Kerr KG, Snelling AM. *Pseudomonas aeruginosa*: a formidable and ever-present adversary. *J Hosp Infect* 2009; 73: 338-344.
2. World Health Organization (WHO) (2024). WHO bacterial priority pathogens list, 2024: Bacterial pathogens of public health importance to guide research, development and strategies to prevent and control antimicrobial resistance [Internet]. Geneva: World Health Organization; [cited 2026 Jul 18]. Available from: https://www.who.int/publications/i/item/9789240093461
3. Kuddus MA, Paul AK. Global Dynamics of a Two-Strain Disease Model with Amplification, Nonlinear Incidence and Treatment. *Iran J Sci* 2023; 47: 259-274.
4. Pang Z, Raudonis R, Glick BR, Lin TJ, Cheng Z. Antibiotic resistance in *Pseudomonas aeruginosa*: mechanisms and alternative therapeutic strategies. *Biotechnol Adv* 2019; 37: 177-192.
5. Salehibarmi M, Siroosi M. Effect of supplementation on biofilms and antibiotic efficacy against *Pseudomonas aeruginosa*. *Iran J Microbiol* 2025; 17: 861-874.
6. Majeed HT, Aljanaby AAJ. Antibiotic Susceptibility Patterns and Prevalence of Some Extended Spectrum Beta-Lactamases Genes in Gram-Negative Bacteria Isolated from Patients Infected with Urinary Tract Infections in Al-Najaf City, Iraq. *Avicenna J Med Biotechnol* 2019; 11: 192-201.
7. Markley JL, Wencewicz TA. Tetracycline-Inactivating Enzymes. *Front Microbiol* 2018; 9: 1058.
8. Liu LK, Abdelwahab H, Del Martin Campo JS, Mehra-Chaudhary R, Sobrado P, Tanner JJ. The Structure of the Antibiotic Deactivating, N-hydroxylating Rifampicin Monooxygenase. *J Biol Chem* 2016; 291: 21553-21562.
9. Li Y, Zhao L, Pu X, Geng B, Liu W, Gao J, et al. Flavin-dependent monooxygenases as versatile biocatalysts in biomanufacturing: mechanisms, engineering, and applications. *Biotechnol Biofuels Bioprod* 2026; 19: 42.
10. Kim DW, Thawng CN, Lee K, Wellington EMH, Cha CJ. A novel sulfonamide resistance mechanism by two-component flavin-dependent monooxygenase system in sulfonamide-degrading actinobacteria. *Environ Int* 2019; 127: 206-215.
11. Ceccoli RD, Bianchi DA, Rial DV. Flavoprotein monooxygenases for oxidative biocatalysis: recombinant expression in microbial hosts and applications. *Front Microbiol* 2014; 5: 25.
12. Gonzalo G de, Mihovilovic MD, Fraaije MW. Recent developments in the application of Baeyer-Villiger monooxygenases as biocatalysts. *Chembiochem* 2010; 11: 2208-2231.
13. Tolmie C, Smit MS, Opperman DJ. Native roles of Baeyer-Villiger monooxygenases in the microbial metabolism of natural compounds. *Nat Prod Rep* 2019; 36: 326-353.
14. Riebel A, Dudek HM, Gonzalo G de, Stepniak P, Rychlewski L, Fraaije MW. Expanding the set of rhodococcal Baeyer-Villiger monooxygenases by high-throughput cloning, expression and substrate screening. *Appl Microbiol Biotechnol* 2012; 95: 1479-1489.

15. Jacewicz A, Schnell R, Lindqvist Y, Schneider G. Crystal structure of the flavoenzyme PA4991 from *Pseudomonas aeruginosa*. *Acta Crystallogr F Struct Biol Commun* 2016; 72: 105-111.
16. Langendonk RF, Neill DR, Fothergill JL. The Building Blocks of Antimicrobial Resistance in *Pseudomonas aeruginosa*: Implications for Current Resistance-Breaking Therapies. *Front Cell Infect Microbiol* 2021; 11: 665759.
17. Green MR, Sambrook J (2012). Molecular Cloning: A Laboratory Manual. 4th ed. Cold Spring Harbor Laboratory Press. Cold Spring Harbor, NY.
18. Rose RL (2002). Measurements of flavin-containing monooxygenase (FMO) activities. In: Current Protocols in Toxicology. John Wiley & Sons, Chapter 4, Unit 4.9, pp. 4.9.1-4.9.11.
19. Orru R, Pazmiño DET, Fraaije MW, Mattevi A. Joint functions of protein residues and NADP(H) in oxygen activation by flavin-containing monooxygenase. *J Biol Chem* 2010; 285: 35021-35028.
20. Miri M, Yazdianpour S, Abolmaali S, Darvish Alipour Astaneh S. Exogenous Production of N-acetylmuramyl-L Alanine Amidase (LysM2) from Siphoviridae Phage Affecting Anti-Gram-Negative Bacteria: Evaluation of Its Structure and Function. *Avicenna J Med Biotechnol* 2022; 14: 46-53.
21. van Berkel WJ, Kamerbeek NM, Fraaije MW. Flavoprotein monooxygenases, a diverse class of oxidative biocatalysts. *J Biotechnol* 2006; 124: 670-689.
22. Schwarz-Linek U, Krödel A, Ludwig F-A, Schulze A, Rissom S, Kragl U, et al. Synthesis of Natural Product Precursors by Baeyer-Villiger Oxidation with Cyclohexanone Monooxygenase from *Acinetobacter*. *Synthesis 2*001; 2001: 947-951.
23. Kamerbeek NM, Olsthoorn AJJ, Fraaije MW, Janssen DB. Substrate specificity and enantioselectivity of 4-hydroxyacetophenone monooxygenase. *Appl Environ Microbiol* 2003; 69: 419-426.
24. Drees SL, Ernst S, Belviso BD, Jagmann N, Hennecke U, Fetzner S. PqsL uses reduced flavin to produce 2-hydroxylaminobenzoylacetate, a preferred PqsBC substrate in alkyl quinolone biosynthesis in *Pseudomonas aeruginosa*. *J Biol Chem* 2018; 293: 9345-9357.
25. Meng N, Li G, Zhang J, Zhu J, Kang X, Duan J, et al. A novel and evolutionarily distinct flavoprotein monooxygenase drives skatole degradation in *Rhodococcus*. *Appl Environ Microbiol* 2026; 92(4): e0022826.
26. Vera A, González-Montalbán N, Arís A, Villaverde A. The conformational quality of insoluble recombinant proteins is enhanced at low growth temperatures. *Biotechnol Bioeng* 2007; 96: 1101-1106.
27. Li YJ, Zheng YC, Geng Q, Liu F, Zhang ZJ, Xu JH, et al. Secretory expression of cyclohexanone monooxygenase by methylotrophic yeast for efficient omeprazole sulfide bio-oxidation. *Bioresour Bioprocess* 2021; 8: 81.
28. Fan X, Widodo WS, Rozeboom HJ, Fraaije MW. Engineered *Escherichia coli* Strains for Flavoprotein Research: From Production of Apoproteins to Incorporation of Flavin Derivatives. *ACS Synth Biol* 2026; 15: 2635-2648.
29. Rehdorf J, Zimmer CL, Bornscheuer UT. Cloning, expression, characterization, and biocatalytic investigation of the 4-hydroxyacetophenone monooxygenase from *Pseudomonas putida* JD1. *Appl Environ Microbiol* 2009; 75: 3106-3114.
30. Fürst MJLJ, Gran-Scheuch A, Aalbers FS, Fraaije MW. Baeyer–Villiger Monooxygenases: Tunable Oxidative Biocatalysts. *ACS Catal* 2019; 9: 11207-11241.
31. Minerdi D, Zgrablic I, Castrignanò S, Catucci G, Medana C, Terlizzi ME, et al. Escherichia coli Overexpressing a Baeyer-Villiger Monooxygenase from *Acinetobacter radioresistens* Becomes Resistant to Imipenem. *Antimicrob Agents Chemother* 2016; 60: 64-74.
32. Gasparrini AJ, Markley JL, Kumar H, Wang B, Fang L, Irum S, et al. Tetracycline-inactivating enzymes from environmental, human commensal, and pathogenic bacteria cause broad-spectrum tetracycline resistance. *Commun Biol* 2020; 3: 241.
33. Catucci G, Zgrablic I, Lanciani F, Valetti F, Minerdi D, Ballou DP, et al. Characterization of a new Baeyer-Villiger monooxygenase and conversion to a solely N-or S-oxidizing enzyme by a single R292 mutation. *Biochim Biophys Acta* 2016; 1864: 1177-1187.
34. Bailleul G, Yang G, Nicoll CR, Mattevi A, Fraaije MW, Mascotti ML. Evolution of enzyme functionality in the flavin-containing monooxygenases. *Nat Commun* 2023; 14: 1042.